STRENGTH AND DEFORMATION TESTING OF RIGID POLYURETHANE SPRAY-ON COATING UNDER INTERNAL PRESSURE

by

Eric J. Steward, B. Sc.

A Practicum Presented in Partial Fulfillment

of the Requirements of the Degree

Master's of Civil Engineering

COLLEGE OF ENGINEERING AND SCIENCE

LOUISIANA TECH UNIVERSITY

December 2008

TABLE OF CONTENTS

ABSTRACT

As the water distribution infrastructure continues to deteriorate across North America, there is a continued need to develop pipeline rehabilitation methods that are cost effective and minimally disruptive on one hand, while minimizing the time a pipe must be taken out of service on the other hand. Spray-on coatings that satisfy the requirements of NSF 61 are one such emerging class of rehabilitation methods. Unfortunately, there appears to be a lack of design guidelines regarding the needed thickness of the coating application to ensure a particular pressure rating at a given factor of safety. This paper reports the findings of an extensive experimental and numerical study aimed at evaluating the internal pressure resistance rating of a spray-on rigid polyurethane coating system. Based on the experimental data an empirical predictive equation was derived for calculating the pressure rating of spray-on coating for a known coating thickness, maximum gap diameter in the host pipe and a safety factor value.

The experimental program consisted of testing polyurethane panels in a specially designed pressure cell with a circular opening to simulate a deteriorated host pipe. The experimental setup was designed to determine both, the burst pressure as well as the amount of deformation the panel underwent as the internal pressure increases. The experimentally measured deformation of the panel during testing was compared with predictions obtained from an analytical model and a finite element simulation in an effort to gain additional insight into the governing failure mechanisms.

The thickness of the panels ranged between 0.14 and 0.42 inches and the size of the opening was 3 or 4.5 inches. Using these controlled variables, along with the measured burst pressure values, a linear regression equation was developed that was found to fit well all of the experimental data. The researchers are currently working on expanding the testing program to other types of spray-on coatings in an attempt of developing a generalized equation that incorporate key mechanical properties of the coating material.

ACKNOWLEDGEMENT

First, I would like to thank my advisor Dr. Erez Allouche for his direction, ideas, and especially his time in guiding this project to completion. I am very grateful to Mr. Jerry Gordon and Mr. Chip Johnson with Sprayroq, Inc. for their kind financial and technical support, without which this project would not be possible. I would like to offer gratitude to Nathan Pettit, Eric Burke, and Eric Slusser at the National Trenchless Technology Research Facility for their time and dedication in preparing and testing samples at all hours of the day and night. Special thanks to Shaurav Alam and Ivan Diaz for guidance in generating the finite element model. Lastly, I would like offer sincere thanks to Dr. Michael Baumert for the design of the experiment, guidance with the instrumentation, but most of all his dedication and camaraderie both here and from a great distance.

1 BACKGROUND AND INTRODUCTION

Over the past 15 to 20 years there has been increased emphasis on the rehabilitation of deteriorating buried municipal pipelines in lieu of replacement with a new pipe, particularly in highly urbanized and environmentally sensitive environments. More recently, there has been an effort to utilize a chemically hardened spray-on coating as a cost effective, fast curing, rehabilitation technique as an alternative to more traditional lining methods. Spray-on coating provides both a corrosion resistant barrier between the pipe and the water along with added structural integrity to the host pipeline. Spray-on coatings used for waterline rehabilitation must meet the NSF 61 Standards to provide safe potable water (Modayil 2005).

Spray-on coatings currently used in waterline rehabilitation are either cement-based or polymer-based as seen in Figure 1 (Morrison 2008). Each category offers different types of coatings depending on the application; which can be altered by using a variety of chemical combinations. In general, each of these spray-on linings is formed by combining two or more substances that when combined, a chemical reaction forms a hardened material shaped to mold along the pipe wall or along pipe deformities.

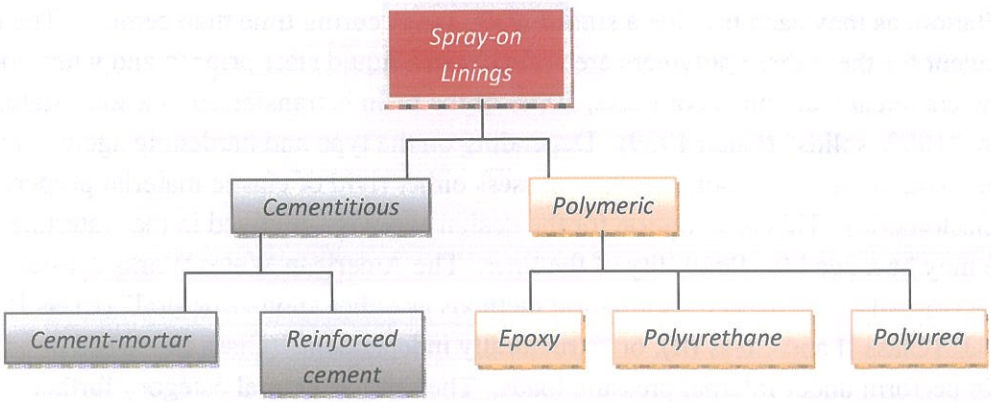

Fig. 1 *Spray-on waterline coatings*

Cement-mortar coating is a mixture of cement, sand, and water that forms a chemically hardened cementitious material installed onto the interior wall of the host pipe (Walker and Guan 1997). While cement coatings have been used for decades as a rehabilitation method, they are only useful in cases where the host pipe has maintained its overall structural integrity. The cement-mortar can provide a successful seal to prevent additional corrosion, increase fluid flow, and address color and odor issues. Cement does not possess a significant amount of tensile strength and therefore cannot provide a pipe with additional structural stability when installed due to the lack of inherent ring stiffness (Bontus, et al. 2005). In an attempt to add tensile strength to cement linings, contractors have introduced steel fibers to cement with some success. This is not to say that cement-mortar coatings cannot bridge small cracks or openings in the host pipe, however, the coating does not possess the ability to provide additional structural stability to the

host pipe if further disintegration occurs. Another major issue with using cement-mortar coatings as an effective rehabilitation method is the relatively long setting time and the relatively slow strength gain rate. Removing waterlines from service for a prolong period is a sensitive issue due to legal requirements to maintain water flow even during maintenance and rehabilitation activities.

When a down time for the waterline must be minimized and more than just a corrosion barrier is required for rehabilitation, a spray-on polymer coating is a reliable alternative. When designed appropriately, polymers can provide a semi-structural component as well as corrosion protection. The term "Polymer" represents a broad class of materials that, by definition, are large covalently bonded chains formed by the combination of smaller molecules. Polymers used for waterline rehabilitation are classified as synthetic "engineered coating/adhesive". These polymers are formed by the combination of a resin and a hardening agent to form a fast curing thermoset material with a crosslinked molecular composition. Depending on the type of adhesive formed, the reaction may require a curing aid such as a catalyst additive or heat (Chemistry Explained: Foundations and Applications 2008).

The three polymeric coatings listed in figure 1 are the most common polymers used for waterline rehabilitation, as they each provide a significantly faster curing time than cement. The resin and curing agent for these three polymers are typically in a liquid state prior to and when combined. Once the chemical reaction is complete, 100% of the resin is transferred to a solid state; hence the term, "100% solids" (Guan 1999). Depending on the type and hardening agent combined with the resin, the resultant polymer may possess either rigid or elastic material properties (also called elastomeric). This is an option for the design chemists involved in the waterline project, as there may be a need for flexibility of the liner. The American Water Works Association (AWWA) classify trenchless rehabilitation methods as either "non-structural" (Class I), "semi-structural" (Class II and Class III), or "structurally independent" (Class IV) based upon their ability to perform under internal pressure loads. The semi-structural category further differentiates between liners with inherent ring stiffness versus those that rely entirely on adhesion to the host pipe to be self-supporting (Bontus, et al. 2005). Polymer coatings are either nonstructural (Epoxy) or semi-structural (polyurethane and polyurea). The semi-structural liners can be applied to the pipe wall in multiple layers called "High Build", and depending on the design and application, they may be a Class II or Class III.

Epoxies are a common type of polymer used in many different applications. This type of polymer is known for possessing strong adhesion to surfaces. Epoxies use a chemical called bisphenol A as the resin along with epichlorohydrin for the hardener (Progressive Epoxy Polymers, Inc. n.d.). These chemicals are typically combined along with a catalyst to elevate the heat and thus inhibit the reaction. Epoxies used for coating waterline are typically 100% solid and are rigid to the point of being almost brittle. The curing time for epoxies are between 7 and 14 days, so they are typically applied as a thin layer (Guan 1999). For this reason, epoxies are commonly not applied using the high-build method and cannot obtain a sufficient or consistent

amount of thickness to provide additional structural support to the host pipe. However, several vendors are currently working on high-build epoxy formulations. To the waterline rehabilitation designers, epoxies are generally considered to be a similar product to cement-mortar liners, as they provide corrosion protection, bridging of small gaps and cracks, and increased flow, but do not enhance the structural stability to the pipe.

Polyurethane and polyurea coating materials are similar and are often placed in the same chemical category. Both the Polyurethane and Polyurea coatings are produced using a isocyanate compound, but each uses a different reacting resin producing a unique molecular chain. The Polyurethane coatings use a Hydroxl (OH)-ending blend called a polyol as the hardened resin, while Polyurea uses amine (H_2N)-ending blend as seen in figures 2 and 3, respectively.

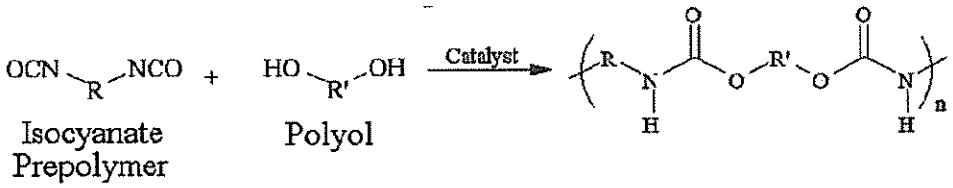

Fig. 2 A General Polyurethane Chemical Reaction (Primeaux 2004)

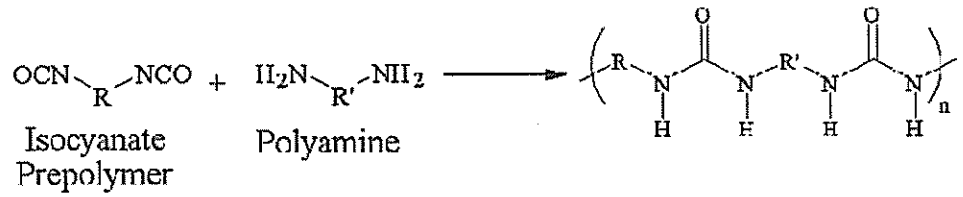

Fig. 3 A General Polyurea Chemical Reaction (Primeaux 2004)

The Polyurethane reaction utilizes a catalyst similar to that of epoxies to produce the resultant material. This reaction produces a 100% solids material within a matter of minutes, so additional layers for high build can be easily applied. For the Polyurea, the reaction with the amines produces a hardened substance extremely quickly, which produces a 100% solids material within a matter of seconds. The installation of polyurea requires the use of a plural component, high pressure, high temperature application system (Primeaux 2004). A catalyst is not necessary using this application technique. Polyurea is suitable for high temperature applications, as it features high heat resistance properties (Guan 1999). Polyurethane coatings can be produced with different types of polyols that can provide a rubber-like property used in pipes that may have flex potential. The urea group chain typically produces an elastomeric material, so if a more rigid material is needed for additional structural stability where flex is not a concern, polyurethane coatings are used. The very quick curing time on both of these spray-on coatings

makes it an attractive rehabilitation method to municipalities looking for short downtime for the potable waterline and force mains.

While each of these polymer coatings offers its own unique advantages, the common characteristic for each of these applications to be successful is to have proper bonding to the host pipe wall, which requires extensive cleaning and drying to provide the best adhesion. There are many techniques for cleaning the inside waterline, with many being proprietary in nature (Gordon 2008).

While there is a significant amount of data regarding curing times, temperature application, and basic mechanical properties, there is currently no standard in North America that provides guidelines to design the proper thickness of spray-on coatings within a pressure pipeline. Because the design thickness will be directly related to the operating pressure of the pipe and the degree of pipe deterioration, this study is aimed at developing an equation that relates failure pressure with the thickness of a coating. The work herein lays the foundation to a more generalized equation that applies to each of the spray-on polymer coatings previously discussed for the case of pressure pipes.

The material used for this study is a commercially available spray-on coating called "Spraywall" generously provided by Sprayroq Inc. "Spraywall" is a rigid 100% solid polyurethane liner that has been used to rehabilitate gravity flow pipelines as well as manholes and other buried structures. This material has recently been approved for potable waterline rehabilitation (Gordon 2008). Sprayroq has performed standard strength testing to determine many of the basic parameters required for proper design, such as Tensile Modulus, Flexure Modulus, and Compressive Strength (Tensile, ASTM D638, Spraywall 2005). This paper presents the results of testing 23 panels of varying thickness subjected to a uniformly incremented pressure until failure. In addition to strength data, deflection measurements of the exposed portion of the panel during testing were obtained. These panel deflection results from the experiment were compared to a numerical model developed using ANSYS (ANSYS, Inc 2007) and predictions from an analytical solution using a linear elastic mechanics equations for deflection of a plate with a clamped boundary (Clamped Circular Plate under Uniformed Load 2008). Combining both the pressure failure data with the deformation data leads to the development of an empirical predictive equation that can be used for design purposes.

2 MECHANICAL PROPERTIES

As previously stated, panels of a 100% solids rigid polyurethane lining material called Spraywall were used as test specimens for this study. This material by design does not possess a significant amount of elastic behavior. The advertised mechanical properties are listed in Table 1.

Table 1: *Spraywall Published Mechanical Properties* (Spraywall 2008)

Flexural Modulus	735,000 psi
Flexural Strength	14,000 psi
Long-term Design life (50 years)	70% of Flexural Modulus
Tensile Modulus	425,000 psi
Tensile Strength	7,450 psi
Elongation	2% at Failure
Density	87 pcf
Hardness-Shore D	90

Because the material has a very high flexural modulus when compared to the tensile modulus, shear will be considered as the main mode of failure, thus the tensile modulus will be the main mechanical property used in the comparative models. Initially, the published tensile modulus value given by an independent testing laboratory dated 2005 was used for modeling (Tensile, ASTM D638, Spraywall 2005). Due to many possible variations, such as changes in resin components, mixing procedures, etc., the tensile modulus value was investigated further. In an effort to remove as much uncertainty as possible, a series of tests were performed in accordance with ASTM D638 to determine the stress versus strain relationship of the material used in the construction of the panels. Coupon samples were cut from both a tested panel and an untested panel in lateral and longitudinal directions. The samples were then tested using an ADMET universal testing machine with a capacity of 2500 pounds. The data was recorded and compiled to form the graph shown in figure 4.

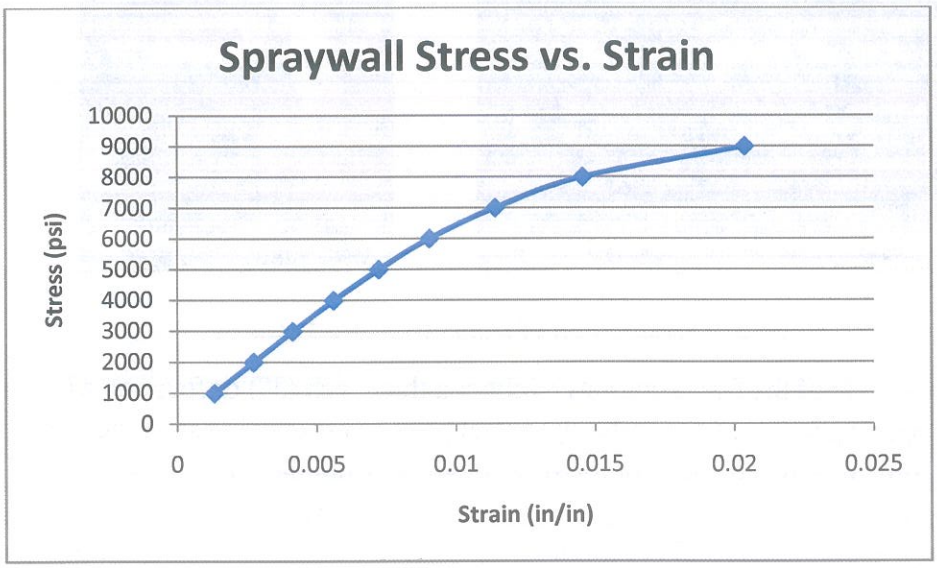

Fig. 4 *Nonlinear Stress versus Strain relationship for Spraywall*

The coordinates of the nine points displayed on Figure 4 were used in the nonlinear material properties portion of the modeling detailed in Section 5. A value of 0.3 is assumed for the Poisson's ratio of the material. This assumption was not confirmed by testing, and may be a conservative value due to the low elongation values presented in the ASTM D638 tests.

3 EXPERIMENTATION

3.1 Apparatus and Experimental Set-up

A testing frame was designed and built by Dr. Mike Baumert for this project. The testing frame consists of two main components; the pressure side and the opening side. The pressure side of the frame is designed to apply a uniform pressure to one side of the panel (Fig. 5). The opening side of the frame contains a circular opening, which simulates a deficiency in the host pipe wall. This opening is the region of the panel where the failure occurs. Both portions of the frame contain a rigid formation of rectangular tube steel attached to a machined flat steel plate (Fig. 6). On the pressure side, the steel plate has a welded steel extension collar that creates a 24" x 24" x 1" cavity where the water pressure will form. This collar has a ⅝" x ¾" square groove machined inside of the bolt pattern to fit a ¾" x ¾" rubber quad-seal (Fig. 5). The remaining ⅛" seal above the groove assists in maintaining the pressure inside the cavity by eliminating any minor deformities in the panel. Inlet and outlet ports are also installed on this collar.

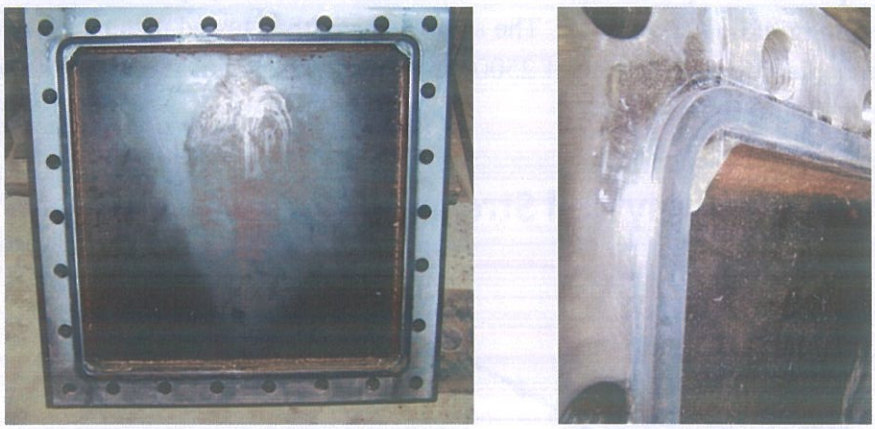

Fig. 5 *Pressure half of frame with quad-seal*

The opening side of the frame consists of either a three inch (3") or four and a half inch (4.5") diameter opening in the center of the rigid steel plate. This opening simulates a portion of material either heavily corroded or missing altogether from the host pipe wall. The two halves of the frame are connected using 26 threaded one inch rods, washers, and nuts. The nuts are tightened to approximately 150 ft-lbs of torque to create a proper seal for the pressure volume. The choice of 150 ft-lbs of torque was made by trial and error, as more torque damaged the quad-seal material.

Fig. 6 *Assembled Testing Frame with Panel*

A pressure supply system was designed to provide up to 1000 psi of water pressure to the frame. The system consists of a high pressure nitrogen tank supplying pressure to an interface chamber which in turn pressurizes the water within the cavity on the pressure side of the frame. A series of regulators, gauges, and relief valves are installed for safety and pressure regulation (Fig. 7). The water side of the interface chamber is connected to the top input port of the pressure cavity, while a pressure transducer is installed on the bottom. The location of the pressure transducer along the cavity is not significant as the head pressure is negligible compared with the high pressures utilized in the tests. To measure the deformation of the exposed panel at the opening as pressure increases, a pivot system was designed to transfer the movement of the panel to a Linear Variable Displacement Transducer (LVDT) (Fig. 8). This pivot system uses a thin threaded rod in contact with the panel at the center of the opening. The rod is held in place by the spring tension from the LVDT piston through the pivot bar. This system protects the LVDT from damage when panel failure occurs. During testing, data from both the LVDT and the pressure transducer is collected using an Agilent data acquisition unit. All testing was performed at the Trenchless Technology Center (TTC) at Louisiana Tech University.

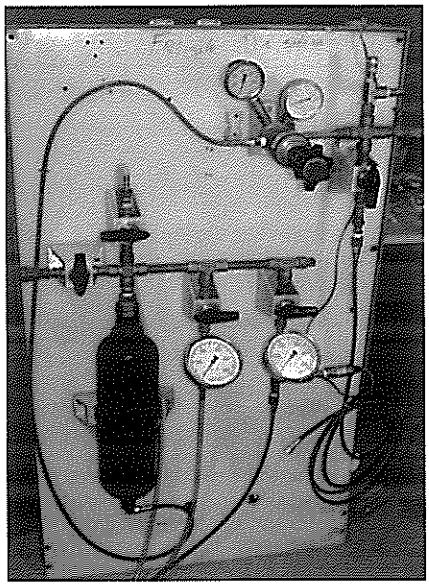

Fig. 7 Pressure supply system with Interface Chamber

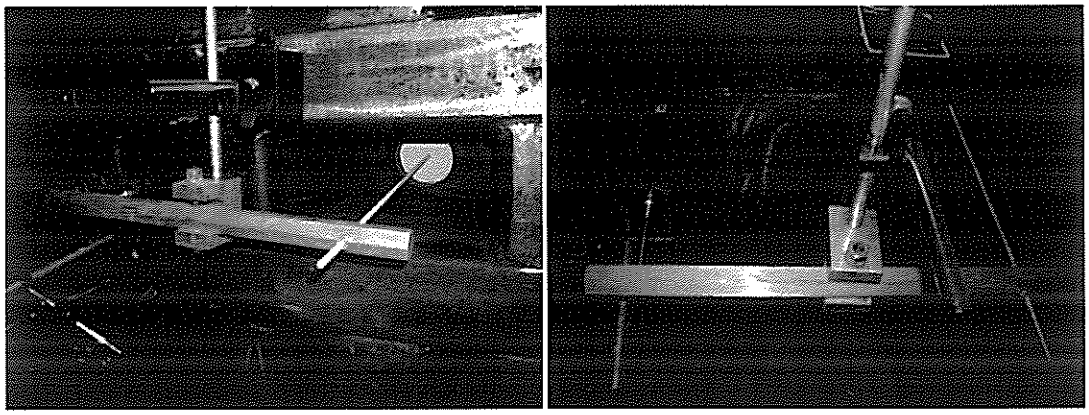

Fig. 8 LVDT installed at panel opening (left: side view, right: top

3.2 Sample Preparation

The experimental portion of this research was conducted on 31 inch square panels of the Polyurethane material. Flat plates were used to simplify the testing apparatus, plus the majority of current applications involve the coating of chambers and large diameter pipes to allow the material to be applied by a human. Sprayroq provided a series of panels with thickness ranging from 0.14 inch to 0.42 inch. A portion of the panels received had minor crevices along edge due to the manufacturing process (Gordon 2008). These minor deformities were located along the gasket seal which generated leaks, so the deformities were filled and sanded smooth using automobile body repair compound. To accommodate the 26 threaded rods required to assemble

the testing frame, 1-⅛ inch holes were drilled into the panel along the edge using a steel frame template (Fig. 9).

Fig. 9 *Panel 6 after drilling and preparation*

3.3 Testing Procedure

Once the panels were prepared and installed into the frame, the transducers were installed and the data acquisition system was powered to begin acquiring data. The pressure cavity was then filled with water to evacuate the air. Once the cavity was filled, the pressure system was transferred to the nitrogen side of the interface chamber to begin applying pressure to the water behind the panel. The pressure was applied in 50 to 100 psi increments with approximately 60 seconds between increments to allow the pressure to stabilize and allow for uniform distribution of the load across the panel. These increments of pressure were applied until failure occurred. This process was repeated for 12 panels using a 3" diameter circular opening and 11 panels with a 4-½" diameter opening.

4 FAILURE ANALYSIS

4.1 Mode of Failure

In each of the 23 tests, rupture was sudden and violent with no audible warning. Due to the high pressures being used, there was no visual observation of the failure, so there is no evidence that failure was about to occur. The material failed in a concentric fashion with respect to the opening walls. Fragments from the panel were collected and pieced together to its original shape. Visual inspection of the fragments indicated that the material assumed little or no permanent deformation throughout the test (Fig. 10). The outer edge of the puncture holes and

the fragments of the material have an angular shape. This shape is indicative of classical punching shear failure, where the failure plane occurs at approximately 45 degree inclination angle to the surface of the panel (Fig. 11) (ACI-318-05 2005). Combining the fact that the fragments fit together with no sign of permanent deformation with the visual observation of the angled failure suggests that the failure mode of this material was a classic punching shear failure with little, if any, bending failure component.

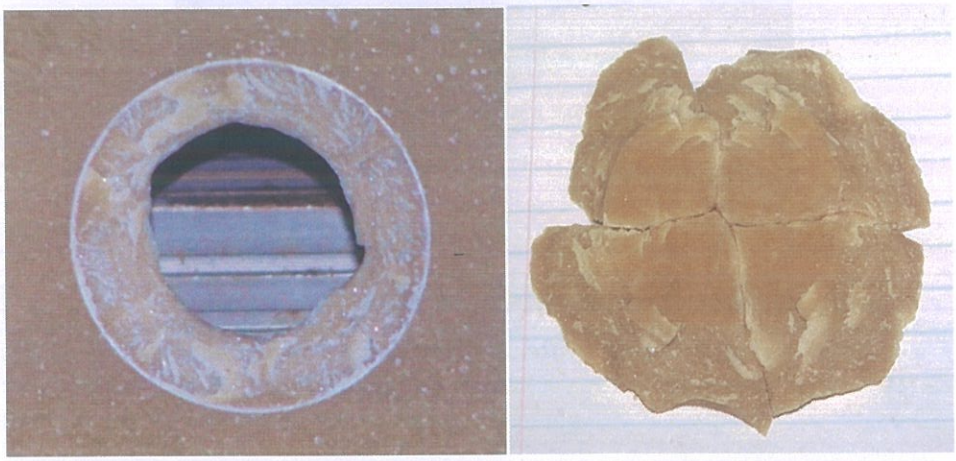

Fig. 10 *Puncture Hole and Fragments*

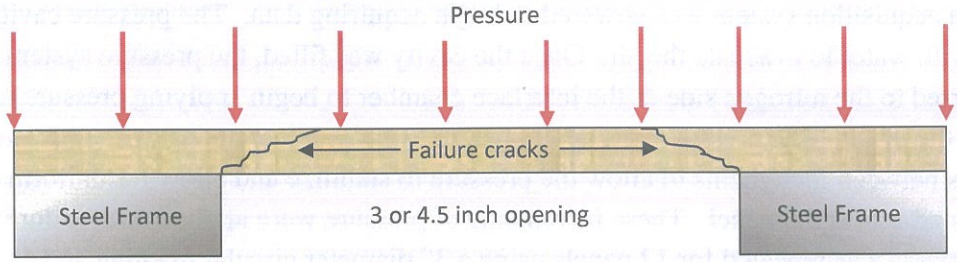

Fig. 11 *Illustration of Punching Shear Cracks, side view*

Another observation is that the failure did not take the form of a plug removed from the panel, but rather several fragments that fail simultaneously. This indicates there is a stress concentration at the center of the circular opening, which is expected based on the finite element simulation. More information on the finite element model is provided in a later section.

4.2 Relationship between failure pressure and panel thickness

Following the disassembly of the test cell and removal of the tested panel, a micrometer was used to measure the thickness of the panel just inside the failure hole at several locations. The average of these measurements was used for all further analysis. It became immediately obvious that the failure pressure was directly related to the thickness of the material. Also, as the opening

size was enlarged, failure pressures decreased for panels with the same thicknesses, as would be expected considering the increase in unsupported panel surface area. Figure 12 provides a comprehensive visual display of the failure pressure and thickness relationship for all panels tested. The trend lines generated from the results are nonlinear, with steeper slopes as thickness increases.

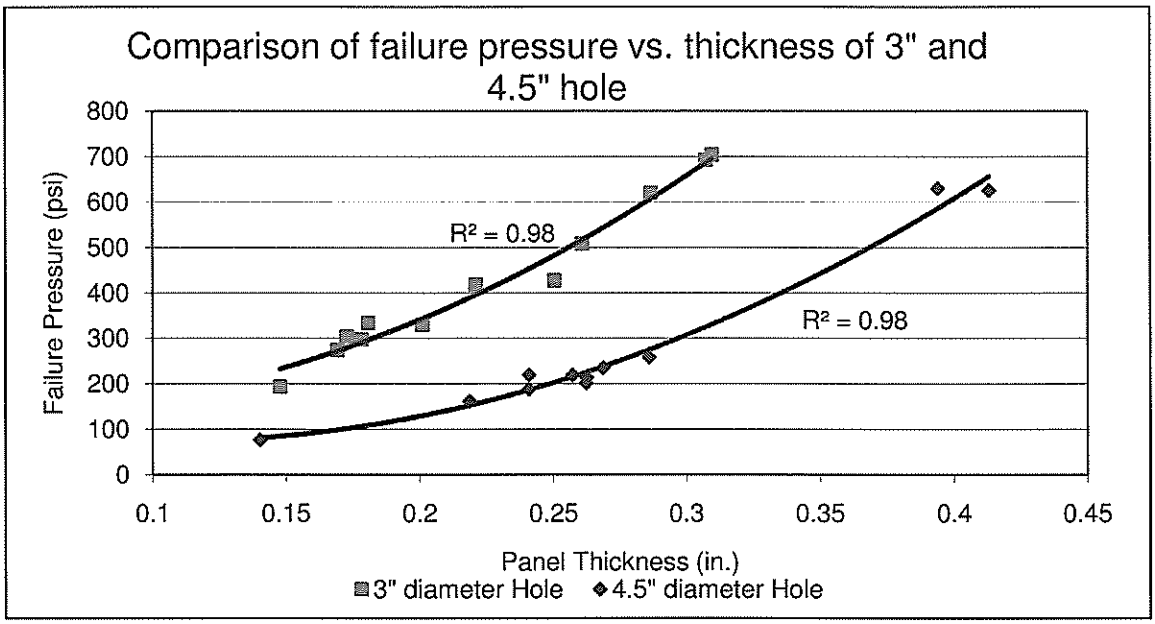

***Fig. 12** Plot of panel test results*

4.3 Development of Prediction Equation

As discussed previously, a design standard dedicated to spray-on polyurethane lining for rehabilitation of pressure pipes does not currently exist. In an effort to develop a predictive equation, the ASTM standard used to design Cured-In-Place Plastic (CIPP) lining was investigated. CIPP is a technique of pipeline rehabilitation that uses a resin impregnated felt tube installed into the host pipe and cured. Unfortunately, implementing the properties of this material into the ASTM F1216 equations X1.6 or X1.7 did not provide reasonable output, as the output thicknesses from these were extremely small regardless of the hole or pipe size (ASTM International 2003). The ASTM F2207 Interactive stress model provided similar results to the F1216. One possible reason the ASTM standards are not compatible with the Polyurethane coating is that the mode of failure for the polyurethane liner is shear versus the CIPP liners which is based on localized bending due to increased strain capability of the elastomeric properties. The CIPP material possesses 3 to 5 times more strain capability under loading which allows for biaxial bending to occur (ASTM International 2006). Because the polyurethane liner is much larger tensile and flexural modulus than that of CIPP, the failure is an instantaneous shearing of fibers. The ASTM F2207 interactive stress model does not comply for this same reason.

A Linear Regression Model was used in an attempt to develop a predictive equation. Linear regression is a statistical approach combining experimental data for the development of a relationship between input variables and the output response (Montgomery 2005). This type of model is purely empirical so data can be added to enhance the accuracy of the equation. Material properties are not included in the development of this equation because this equation is only valid for materials with similar properties to that of 'Spraywall'.

The failure pressures and opening sizes were considered the regressor variables, meaning they were the input values to the equation. The thickness was the response variable that the equation was to predict. The thought was to input the design pressure and an estimated opening size for the host pipe, and the equation produces a required thickness for the spray on lining. The data was arranged in matrices and then manipulated to produce regression coefficients called Betas (Montgomery 2005). The software tool MATLAB was used for the matrix calculations which produced the following equation (see Appendix 'A' for MATLAB code):

$$Thickness\ (in) = -0.1378 + [0.0004 * Pressure\ (psi)] + [0.0684 * Opening(in)] \quad \textbf{\textit{Eqn. 1}}$$

For verification, the test data was inserted into this equation to produce Table 2, which displays the errors between the predicted thickness and the actual thicknesses. The errors are considered acceptable because the predicted values are more conservative than the actual values.

Table 2 *Verification of predicted model by percent error*

Failure Pressure (psi)	Opening (in)	Actual Thickness (in)	Predicted thickness (in)	Absolute Value of delta (in)	Error (%) [T_P - T_A/T_A x 100]
193.0	3	0.148	0.145	0.0032	2.2
274.0	3	0.169	0.177	0.0078	4.6
305.0	3	0.173	0.189	0.0166	9.6
298.0	3	0.178	0.187	0.0084	4.7
334.0	3	0.181	0.201	0.0204	11.3
330.0	3	0.201	0.199	0.0016	0.8
418.0	3	0.221	0.235	0.0136	6.2
427.4	3	0.250	0.238	0.0121	4.8
508.0	3	0.261	0.271	0.0097	3.7
619.9	3	0.287	0.315	0.0288	10.0
691.5	3	0.307	0.344	0.0367	12.0
703.0	3	0.310	0.349	0.0390	12.6
76.5	4.5	0.140	0.201	0.0604	43.0
161.6	4.5	0.219	0.235	0.0161	7.4
188.4	4.5	0.241	0.245	0.0045	1.9
219.2	4.5	0.241	0.258	0.0168	7.0
219.2	4.5	0.257	0.258	0.0005	0.2

202.0	4.5	0.262	0.251	0.0115	4.4
214.2	4.5	0.262	0.256	0.0067	2.6
235.0	4.5	0.269	0.264	0.0047	1.7
258.6	4.5	0.286	0.273	0.0126	4.4
630.0	4.5	0.394	0.422	0.0280	7.1
626.0	4.5	0.413	0.420	0.0073	1.8

Rearranging the equation to solve for pressure and adding a factor of safety (N), produces the following empirical equation:

$$Pressure\ (psi) = 344.5 - [171 * Opening(in)] + \frac{[2500 * thickness\ (in)]}{N} \qquad \textit{Eqn. 2}$$

Equation 2 produces a relatively accurate, yet conservative value of the needed minimum thickness of the polyurethane spray-on coating for a given set of design pressure and opening size values. There should be a number of restrictions placed on the use of this equation for design purposes:

- Only a liner with similar material properties to the material tested for this investigation can be considered.
- A minimum applied thickness should be used for any installation, as the results from this equation can be very small or negative when very small opening sizes are used. Further discussion may be required, but an initial value of 0.150 inches is proposed.
- The opening size used in this equation should not exceed the diameter of the host pipe.
- Consideration should be given for the future deterioration of the host pipe and the opening size chosen should reflect that choice.
- Recommended value for N is 2.0.

5 COMPARISON OF EXPERIMENTAL, NUMERICAL, AND ANALYTICAL RESULTS

There is a growing need to develop a design approach for spray-on coating applications that can be used to predict deflection, thus enhancing the predictive equations for a given thickness. This section provides the results of the measured experimental deflections and compares these with theoretical and numerically simulated results.

5.1 Experimental Measurements - Deformation

The deformation data was electronically retrieved from the LVDT for 19 of the 23 tests performed. As expected, the lower thickness of the panel, the more deformation occurred. The thinner the material, the more it tends to bend as the pressure is increased. The deformation at the failure pressure were compared to the thickness, and revealed that the material outer displacement at failure is approximately 54% ± 26% its thickness. The relationship of the

deformation and the thickness at pressure throughout the range are displayed in figures 13a and 13b for the 3" and 4.5" openings, respectively.

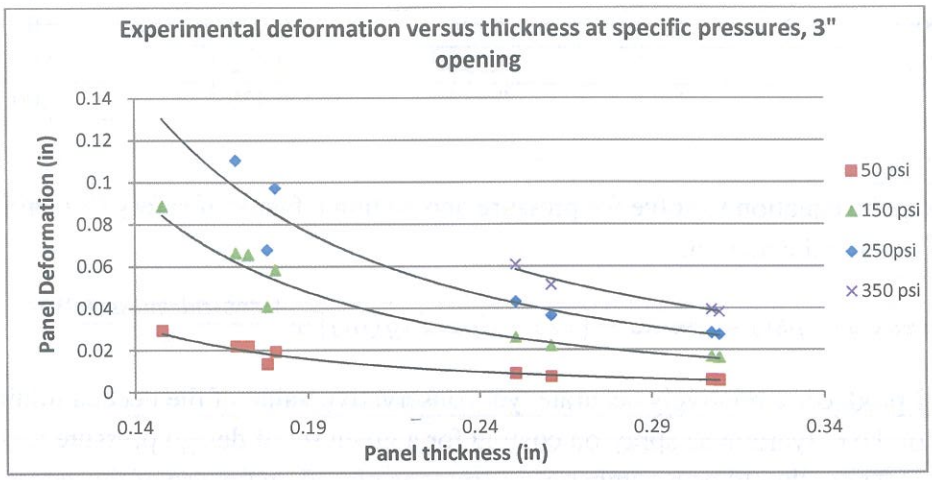

Fig. 13a *Deflection versus thickness plots at specific pressures for 3" opening*

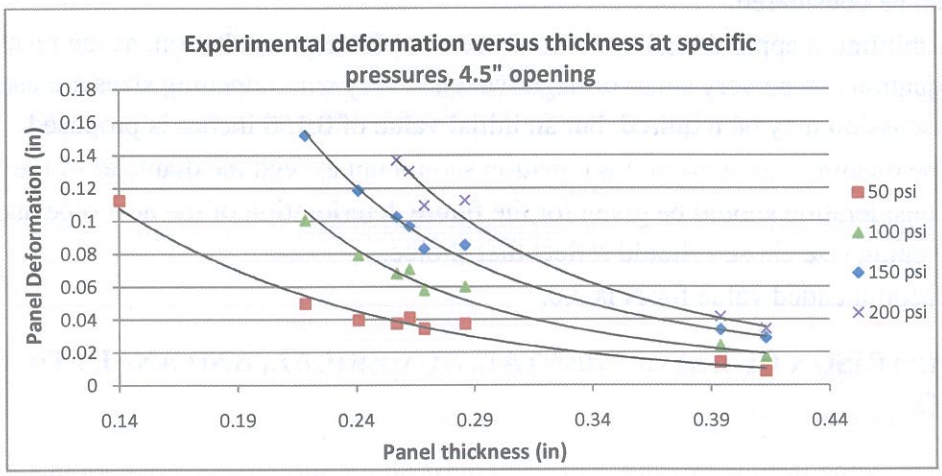

Fig. 13b *Deflection versus thickness plots at specific pressures for 4.5" opening*

The trend lines on the graphs are power equations and provide relatively accurate data when used for prediction, with R^2 equaling 0.94 to 0.95. The equation of the 150 psi trend line for the 3" opening is shown as equation 3 and the equation of the 150 psi trend line for the 4.5" opening is shown as equation 4. The equations for all trend lines are presented in Appendix 'B'. There was an attempt to use existing modeling tools to predict these deformations as is discussed in the next section.

$$Deformation\ (in) = 0.0011 * Thickness\ (in)^{-2.25} \qquad \textit{Eqn. 3}$$

$$Deformation\ (in) = 0.003 * Thickness\ (in)^{-2.58} \qquad \textit{Eqn. 4}$$

5.2 Analytical Solution

Classical elastic theory typically treats deflection as very small when compared to the size of the material. In these small deflections, the material can be treated as pure bending by lateral loading (Li 2005). The maximum deflection will be considered for this evaluation. This deflection will be located at the center of the exposed plate.

Consider the origin of coordinates of a non-deformed plate, where r is the radial distance between a point on the plate and its center, r_o is the radius of the plate, and η represents the deflection in the downward direction. The uniform pressure applied is P, as illustrated in figure 14.

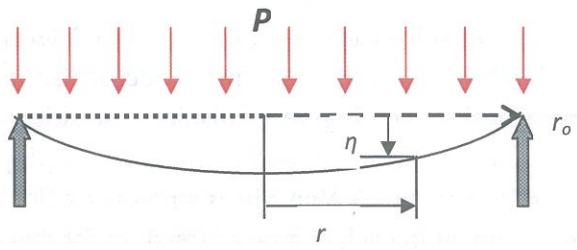

Fig. 14 *Deflection of clamped plate through of axis of symmetry*

Applying the linear elastic theory with the pure bending assumption, the relationship between the plate deflection η and the load P is

$$\eta = \frac{Pr_o^4}{64D}\left[1 - \left(\frac{r}{r_o}\right)^2\right]^2 \qquad \textit{Eqn.5}$$

where D is referred to as the plate rigidity, which involves the Modulus of Elasticity E, Poisson's ratio v, and plate thickness h (Li 2005). D is given by

$$D = \frac{Eh^3}{[12(1-v^2)]} \qquad \textit{Eqn. 6}$$

Because the maximum deflection occurs at the center of the plate where $r_o = r$, the linear elastic equation simplifies to be

$$\eta_{max} = \frac{Pr_o^4}{64D} \qquad \textit{Eqn. 7}$$

5.3 Finite Element Analysis

A typical method for analysis of deflections of materials under loading is the Finite Element Method (FEM). Typically, FEM is a software program designed using the basic stiffness equation $[K]\{d\}=\{P\}$, where $[K]$ is the stiffness matrix, $\{d\}$ is the nodal displacement vector, and $\{P\}$ is the load vector (Li 2005). The software is then used to determine the displacement, stress, strain, or forces on any element location of a structure.

The commercial finite element software ANSYS was used for this project to determine the maximum deflections of the plate. The complete polyurethane panel was generated using the SOLID45 element. The SOLID45 is an eight node element with 3 degrees of freedom at each node (ANSYS, Inc 2007). Each element on the face of the plate, excluding the elements in a three inch diameter location in the center, had restricted movement in direction parallel to that of the applied load, simulating the restriction of the panel against the rigid steel plate. These elements were allowed to move freely in both lateral and longitudinal directions. The elements within the three inch diameter opening were allowed to move freely in all directions, similar to the actual experimental set-up. A uniformed pressure was applied to the surface in increments to acquire the necessary data.

The simulation was then performed for each panel thickness to determine the deformation at the experimentally determined failure pressure. Intermediate deformation values were collected at various pressures for further evaluation. Figure 15 displays the side view with an exaggerated deformation plot at the center of the panel, as well as an image displaying the Von Mises stresses throughout the plane view of the panel. A Von Mises stress is a calculated value that combines the stresses felt by a single element in each degree of freedom for that element. The plot clearly shows the concentration of stress at the center of the opening, as well as the outer diameter of the opening, as expected. It is also interesting to point out that the plot clearly indicates the influence of lateral stress and strain on elements beyond the opening area, which is not considered by the mathematical elastic theory equations used in Section 4.1.

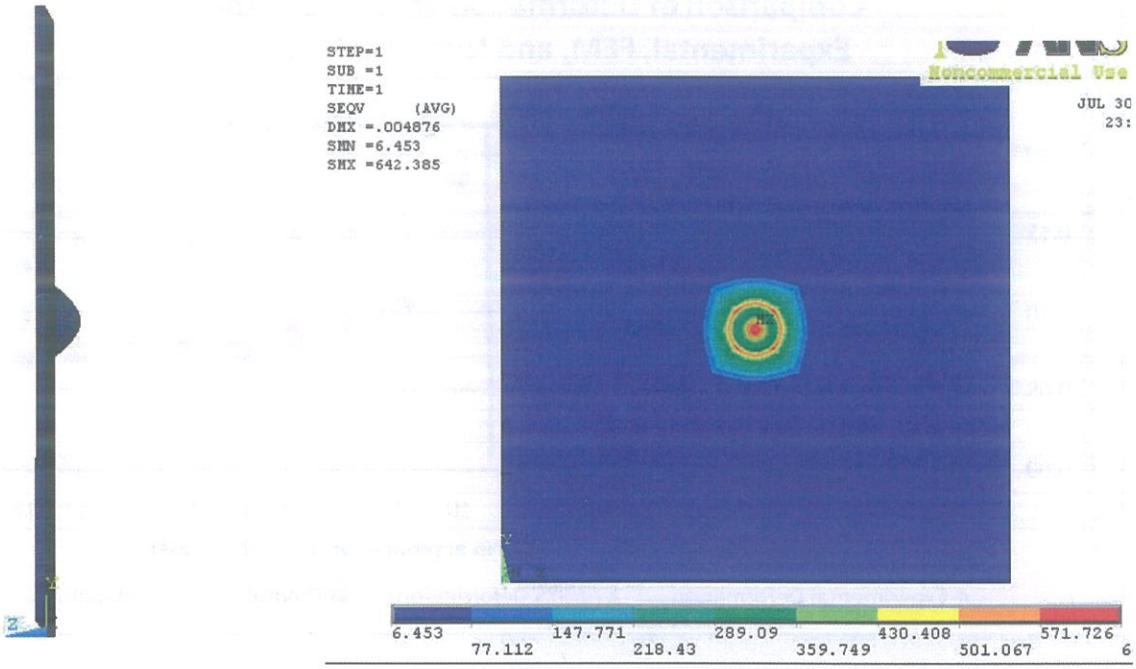

Fig. 15 *ANSYS Deformation and Von Mises Stress Plots (Panel 11 at 50 psi)*

5.4 Comparison of Observed and Predicted Deformations

This analysis begins with an idealized analytical solution as a first attempt to predict the measured deformation of each panel based on thickness. After comparing these results with the experimental data, it became evident that the model predictions do not agree well with the observed values. Next, a finite element model was constructed. While results from the finite element analysis model are in closer agreement with the measured values, there is still a relatively large error. Figure 16 provides a visual display of the comparison between the experimental data and the two models previously described. The horizontal axis is the number given to the panels tested and they are arranged in increasing order by thickness and opening size. The vertical axis is the maximum deformation of the panel, just before failure.

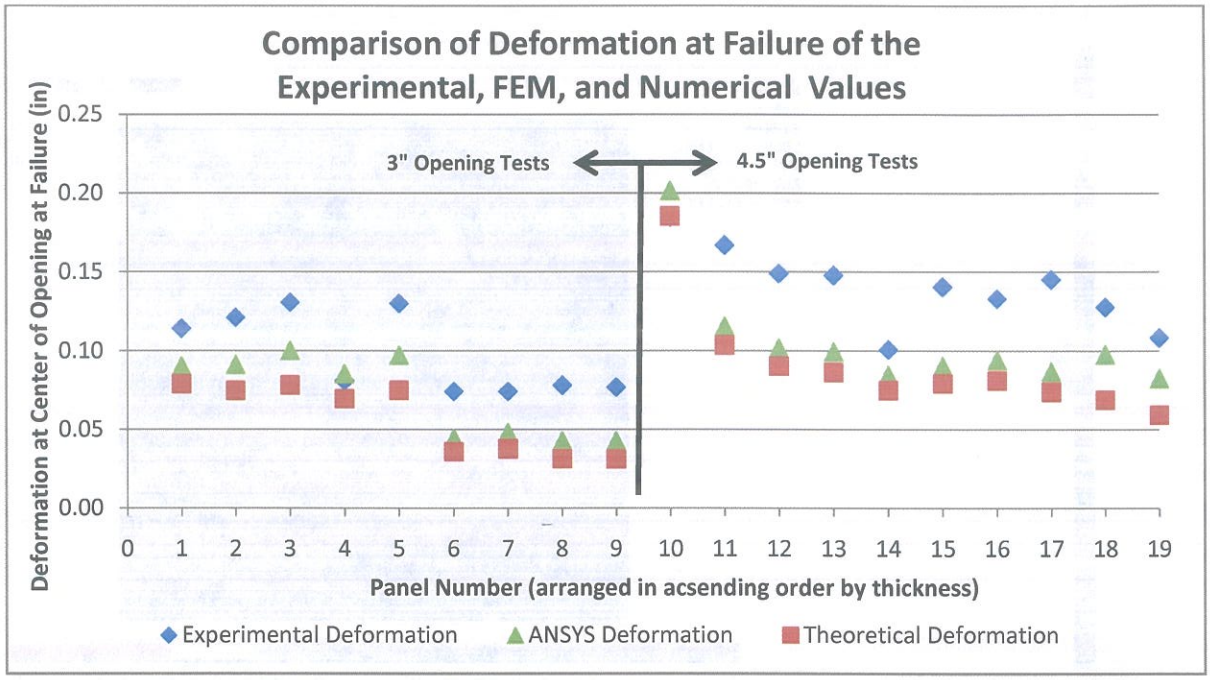

Fig. 16 *Plot of the maximum deformation for each panel compared to the numerical and finite element models at the same pressures*

The trend on the plot indicates that as the thickness of the panel increases, the deformation decreases. This is expected, as there is more material structure to support across the opening. Only 19 of the 23 panels were used for this analysis because the other four panels provided bogus deformation data. The experimentally measured deformation is constantly greater than the predicted deformation. However, the analytical solutions and the numerical solutions appear to be in close agreement in all cases. Furthermore, the difference between the experimental data and the predicted values appears to be relatively constant. Thus, some uncertainty exists as to the accuracy of the experimental data. One standing question is with respect to the mechanical slack in the experimental setup. While some adjustment was made to account for the slack, it is difficult to completely eliminate this source of experimental error. Additional work is needed to determine if either the predictive models used are over simplified and fail to capture the behavior of the panel during loading, or an aspect of the experimental setup amplifies the displacement measurements.

Table 3 List of deformations calculated and measured along with the associated errors

Panel #	Opening	Thickness	Failure Pressure	Experimental Deformation	ANSYS Deformation	Theoretical Deformation	ANSYS Error	Theoretical Error
1	3	0.148	193.0	0.1141	0.0904	0.0790	20.8%	30.8%
2	3	0.169	274.0	0.1212	0.0914	0.0747	24.6%	38.4%
3	3	0.173	305.0	0.1308	0.1000	0.0781	23.5%	40.3%
4	3	0.178	298.0	0.0809	0.0852	0.0696	5.3%	14.0%
5	3	0.181	334.0	0.1302	0.0972	0.0749	25.3%	42.5%
6	3	0.250	427.4	0.0742	0.0441	0.0359	40.6%	51.5%
7	3	0.261	508.0	0.0742	0.0481	0.0378	35.2%	49.1%
8	3	0.307	691.5	0.0780	0.0428	0.0315	45.1%	59.6%
9	3	0.310	703.0	0.0769	0.0428	0.0313	44.4%	59.3%
10	4.5	0.140	76.5	0.1848	0.2015	0.1855	9.0%	0.4%
11	4.5	0.219	161.6	0.1669	0.1155	0.1036	30.8%	38.0%
12	4.5	0.241	188.4	0.1492	0.1017	0.0902	31.8%	39.5%
13	4.5	0.257	219.2	0.1479	0.0994	0.0862	32.8%	41.7%
14	4.5	0.262	202.0	0.1006	0.0844	0.0749	16.1%	25.6%
15	4.5	0.262	214.2	0.1407	0.0904	0.0792	35.7%	43.7%
16	4.5	0.269	235.0	0.1331	0.0940	0.0810	29.4%	39.1%
17	4.5	0.286	258.6	0.1453	0.0866	0.0739	40.4%	49.1%
18	4.5	0.394	630.0	0.1278	0.0977	0.0689	23.6%	46.1%
19	4.5	0.413	626.0	0.1083	0.0826	0.0594	23.8%	45.2%
Average							28.3%	39.7%

6 CONCLUSION AND FUTURE WORK

The goal of this project was to develop a prediction equation that could aid in the determination of spray-on liner thickness to be applied to pipes subjected to internal pressure. Using the results from the testing, an empirical design equation was developed to determine the needed thickness of a polyurethane lining given the internal operating pressure of the pipe and an estimated damage zone in the host pipe. This study also provides pertinent data regarding the amount of deformation or bulge the material would undergo under pressure.

6.1 Improving the Prediction Equation

Spray-on pipeline coatings come in a variety of chemical properties and combinations that would possess a range of mechanical characteristics. Further testing should be performed using different types of coatings to add elastic and flexure modulus as additional regressor variables to the equation.

The next phase of this project can be performing similar pressure testing on lined pipe of varying diameters and thicknesses. This will slightly alter the geometry of the opening that can possibly alter the results. Adding the different tensile modulus and performing these full-scale lined pipe testing can then be developed into a possible standard for the design of polyurethane coatings for pressure pipeline rehabilitation.

6.2 Further Development of Deformation Model

The deformation prediction models require additional investigation. If it is desired to further develop the analytical equations for more accurate prediction of deformation with pressure then the model must utilize a more accurate depiction of the mechanics of the interaction of the liner with the restrictive body, i.e. the host pipe. The theoretical equations used do not take into consideration the strain of the middle plane of the plate (Li 2005). A more elaborate equation that captures the strain is the energy method-first proposed by Timoshenko (Li 2005).

Utilizing the finite element modeling will surely enhance the level of understanding of the liner and host pipe interaction as well as generate accurate movement of the liner under pressure. More investigation must go into improving the design of the model used in this project. Some suggested improvements could be to: a) create a more elaborate 3-dimensional model of the experimental setup, b) determine the Poisson's ratio of polyurethane, and c) compare other program options, such as element type and mesh size.

6.3 Enhancing Experimental Data

During the analysis of the experimental deformation data, it was noticed that there is a level of uncertainty as to the point at which the panel was "seated" onto the steel plate and the bulging of the material began. The LVDT data began at the initial time after the cell was assembled, when no pressure was placed on the pressure side of the panel. Typically, there was a gap between the panel and the steel plate after assembly because the system is in a relaxed state. Once the water pressure was applied to the panel and then the high pressure, the panel was forced against the steel plate. This "slack" on the panel generates an uncertainty of when the material is deforming versus seating. This is one error that should be investigated further for more accurate deformation data.

It would also be beneficial to invest time into accurately determining the Poisson's ratio for this material. Having a verified Poisson's ratio would not only enhance the accuracy of the modeling for deformation comparison, but understanding the strain versus pressure relationship based upon a given opening size could also provide the key to accurately determining the deformation and failure of this material.

BIBLIOGRAPHY

Advameg, Inc. 2008. http://www.chemistryexplained.com/Pl-Pr/Polymers-Synthetic.html (accessed December 3, 2008).

ACI-318-05. *Building Code Requirements for Structural Concrete (ACI 318-05) and Commentary (318R-05).* Farmington Hills, MI: American Concrete Institute, 2005, 430.

"ANSYS, Inc." *Release 11 Documentation.* Pennsylvania, 2007.

ASTM International. "Standard Practice for Cured-in-place Pipe Lining System for Rehabilitation of Metallic Gas Pipe." In *ASTM International Book of Standards, Vol 08.04,* F2207. West Conshohocken: ASTM International, 2006.

ASTM International. "Standard Practice for Rehabilitaion of Existing Pipelines and Conduits by the Inversion and Curing of a Resin-Impregnated Tube." In *Annual Book of ASTM Standards, Vol 08.04,* F1216. ASTM International, 2003.

Bontus, G., M. Brand, K. Oxnar, and J. Gumbel. "Trenchless Rehabilitation Options for Potable Water Systems - the Wave of the Future." *Bridgeing the Gaps, Technological Development to Practical Application.* Saskatoon, Saskatchewan: 57th Annual Conference of the Western Canada Water and Wastewater Association, 2005.

Clamped Circular Plate under Uniformed Load. 2008. http://www.efunda.com/formulae/solid_mechanics/plates/calculators/cpC_PUniform.cfm#Results (accessed July 29, 2008).

Gordon, Mr. Jerry, interview by Eric Steward. *Phone conversation* (July 28, 2008).

Guan, Dr. Shiwei. *Common Questions on 100% Solids Polyurethane Coating.* April 1999. http://www.geocities.com/pucoating/pwsp.htm (accessed November 24, 2008).

Li, Qiuhua. "Large deflection of laminated circular plates with clamped edge and uniform loading." *IMechE,* 2005.

Modayil, Sincy. "Testing and Evaluation of Lining Materials for Drinking Water Pipeline Rehabilitation." In *Water Quality in the Distribution System,* by Bill Lauer and William C. Lauer, 387-410. American Water Works Association, 2005.

Montgomery, Douglas C. *Design and Analysis of Experiments.* 6th. Hoboken, NJ: John Wiley and Sons, Inc., 2005.

Morrison, Robert S. "Water and Force Main Rehabilitation State-of-the-Technology." *EPA Rehabilitation for Wastewater Collection and Water Distribution System Forum.* Edison, N.J., 2008.

Primeaux, Dudley J. "Polyurea vs Polyurethane & Polyurethane/Polyurea: What's the Difference?" *Polyurea Coatings: That Was Then, This Is Now, 2004 PDA Annual Conference.* Tampa: Primeaux Associates, LLC, 2004. 1-20.

Progressive Epoxy Polymers, Inc. *Chemistry of Epoxies, Novolacs, and Polyurethanes.* http://www.epoxyproducts.com/chemistry.html (accessed November 24, 2008).

Spraywall. 2008. http://www.sprayroq.net/content/view/47/68/lang,english/ (accessed August 28, 2008).

Tensile, ASTM D638, Spraywall. Austin: Texas Research Institute, 2005.

Walker, David, and Dr. Shiwei Guan. "Protective Linings for Steel Pipe in Potable Water Service." *'97 NACE Corrosion Prevention Conference.* Houston, 1997.

APPENDIX 'A' MATLAB Linear Regression Code

```
%Eric Steward
%Linear regression of experimental data
%TTC Polyurethane Pressure Project, November 9, 2008

%Build the X Matrix, regressor variables
X = [1,76.5,4.5;1,161.6,4.5;1,188.4,4.5;1,219.2,4.5;1,202,4.5;1,214.2,4.5;
    1,219.2,4.5;1,235,4.5;1,258.56,4.5;1,626,4.5;1,630,4.5;1,193,3;1,274,3;
    1,305,3;1,298,3;1,334,3;1,330,3;1,418,3;1,427.36,3;1,507.99,3;
    1,619.9,3;1,691.53,3;1,702.98,3];

%Build the y Matrix, Vector of Responses
y = [0.140230769;0.2185;0.240833;0.257153846;0.262285714;0.262428571;
    0.240833333;0.268666667;0.286;0.4130625;0.394;0.1478;0.1692;0.1728;
    0.1782;0.1806;0.201;0.221;0.250428571;0.260857143;0.286571429;
    0.307285714;0.309571429];

%Left side of Least Squares estimate of Beta
LPrime = X';
L = LPrime*X;
Linv = inv(L);

%Right side of Least Squares estimate of Beta
R = X'*y;

%Regression Coefficients, Betas
Beta = Linv*R
```

APPENDIX 'B' Trend line Equations from Figures 13a and 13b

Trend line equations for 3" opening graph, figure 13a:

50 psi: $Deformation\ (in) = 0.0004 * Thickness\ (in)^{-2.252}$

150 psi: $Deformation\ (in) = 0.0011 * Thickness\ (in)^{-2.252}$

250 psi: $Deformation\ (in) = 0.0022 * Thickness\ (in)^{-2.132}$

350 psi: $Deformation\ (in) = 0.0037 * Thickness\ (in)^{-1.985}$

Trend line equations for 4.5" opening graph, figure 13b:

50 psi: $Deformation\ (in) = 0.3611 * Thickness\ (in)^{-8.630}$

100 psi: $Deformation\ (in) = 0.0019 * Thickness\ (in)^{-2.662}$

150 psi: $Deformation\ (in) = 0.0030 * Thickness\ (in)^{-2.582}$

250 psi: $Deformation\ (in) = 0.0029 * Thickness\ (in)^{-2.837}$